Taylor & Francis
Taylor & Francis Group

Applied Spectroscopy Reviews

Flow field-flow fractionation hyphenated with inductively coupled plasma mass spectrometry: a robust technique for characterization of engineered elemental metal nanoparticles in the environment

Qingsheng Bai, Yongguang Yin, Yanwanjing Liu, Haowen Jiang, Mengxin Wu, Weidong Wang, Zhiqiang Tan, Jingfu Liu, Myeong Hee Moon & Baoshan Xing

Taylor & Francis
Taylor & Francis Group

Check for updates

Flow field-flow fractionation hyphenated with inductively coupled plasma mass spectrometry: a robust technique for characterization of engineered elemental metal nanoparticles in the environment

Qingsheng Bai[a,b], Yongguang Yin[a,b,c] (iD), Yanwanjing Liu[c], Haowen Jiang[a,b], Mengxin Wu[a], Weidong Wang[d], Zhiqiang Tan[a,b,c], Jingfu Liu[a,b,c], Myeong Hee Moon[e], and Baoshan Xing[f] (iD)

[a]State Key Laboratory of Environmental Chemistry and Ecotoxicology, Research Center for Eco-Environmental Sciences, Chinese Academy of Sciences, Beijing, China; [b]College of Resources and Environment, University of Chinese Academy of Sciences, Beijing, China; [c]School of Environment, Hangzhou Institute for Advanced Study, University of Chinese Academy of Sciences, Hangzhou, China; [d]Department of Basic Science, Southwest University, Chongqing, China; [e]Department of Chemistry, Yonsei University, Seoul, South Korea; [f]Stockbridge School of Agriculture, University of Massachusetts, Amherst, MA, USA

ABSTRACT

Due to the increased applications of engineered elemental metal nanoparticles (EMNPs) in recent years, increased attention has been devoted to their release into the environment. EMNPs pose potential risks to living organisms, including human beings. Hence, the characterization of EMNPs in the environment has gained significant importance. Among the various techniques reported for the characterization of EMNPs, on-line coupling of flow field-flow fractionation with inductively coupled plasma mass spectrometry (F4-ICPMS) has been well established for the simultaneous separation, identification, and quantification of EMNPs, especially in the complex matrices of environmental samples. Thus, this review focuses on the specific advantages of the F4 method, especially the asymmetrical F4 (AF4) and hollow fiber F4 (HF5) methods, in the separation of EMNPs, the general development of AF4-ICPMS and HF5-ICPMS techniques, and recent advances in the application of these hyphenated techniques in examining the occurrence and transformation of EMNPs in the environment. Finally, several perspectives on these techniques have been put forward.

1. Introduction

Engineered nanomaterials have been widely used in electronics, textiles, cosmetic products, food packing and storage, environmental remediation, medicine, and other industries due to their extraordinary physical and chemical properties, such as small size effect, high surface area to volume ratio, surface and interfacial effects, quantum size effect, dielectric confinement effect, and macroscopic quantum tunneling effect.[1–4]

Different classes of nanomaterials exist, among which engineered elemental metal nanoparticles (EMNPs), such as silver nanoparticles (AgNPs), gold nanoparticles (AuNPs), and platinum nanoparticles (PtNPs), contain clusters of reduced metal atoms, making them highly reactive.[5] In practice, they have carved a successful niche in industrial catalysis,[6] energy storage,[7] optoelectronics,[8] and biocidal treatments.[9,10]

The widespread use of products containing EMNPs has made their release into the environment unavoidable. EMNPs migrate and distribute in various environmental media and circulate simultaneously in the entire ecosystem through air, water, soil/sediment, biological systems, and other media. Moreover, EMNPs released into the environment undergo a series of transformations, such as formation of the corona structure, aggregation, redox reactions, and sulfidation, etc.,[11–13] which makes it challenging to completely understand their fate and transport. In addition, EMNPs also actively interact with other coexisting pollutants.[14,15] In our recent study, we showed that AgNPs detoxified As(III) under specific environmental conditions through the oxidation of As(III) to less toxic As(V).[16] Furthermore, we demonstrated that the detoxification ability of AgNPs was closely associated with the size and concentration of AgNPs as well as their solution chemistry. A tons of reported studies have demonstrated that the ecotoxicological risks of EMNPs are strongly correlated with the physicochemical properties of EMNPs, such as composition, particle size, concentration, and stability in environmental and biological matrices.[17–21] To accurately assess the fate of EMNPs in natural environment and to understand the potential risks of EMNPs in depth, analytical techniques for the characterization of EMNPs in complex environmental matrices need to be developed urgently.

Inductively coupled plasma mass spectrometry (ICPMS) is one of the most powerful techniques for the simultaneous determination of the chemical composition and concentration of metal particles and has been applied since the beginning of the 1980s. This is mainly facilitated by high efficiencies of vaporization, atomization, and ionization induced by plasma and the multi-element detection capabilities of the technique with high sensitivity and wide linear range.[22–24] However, conventional ICPMS fails to determine the size of EMNPs, mainly due to its limited resolution to distinguish different particle sizes in an EMNP mixture. As a promising alternative for the determination of the size of EMNPs, single particle ICPMS (SP-ICPMS) with extremely short dwelling periods has evolved. In this technique, the signal is strictly proportional to the size of the particles.[25] However, there is a need to reduce the background signals and improve the transmission of ions in order to achieve higher detection efficiency and detect smaller nanoparticles, which will further help to expand the scope of applications of this technique for the characterization of EMNPs in real environmental samples.[26,27] Hence, further refinement is required to improve the performance of SP-ICPMS and thus enables its widespread use in common laboratories. Therefore, great efforts are being made to overcome the shortcomings of conventional ICPMS for the characterization of EMNPs.

Coupling of ICPMS with flow-based separation techniques facilitates the on-line measurement of the size and concentration of EMNPs. This strategy effectively circumvents problems of labor and time consumption and limited applicability to EMNPs with a wide size distribution for common off-line separation methods, such as centrifugation

and extraction. Size exclusion chromatography (SEC)[28,29] and flow field-flow fraction-ation (F4)[30–32] are two of the most powerful flow-based techniques that have gained considerable interests in the separation and characterization of EMNPs. In contrast to SEC, F4 is applicable to particle sizes in the range of 1 nm to 100 μm, thus covering the entire size range of EMNPs.[33] Moreover, theoretical and experimental studies have shown that the size-based selectivity related to the fractionation ability of F4 is much higher than that of SEC.[34] In SEC columns, the most commonly used stationary phase gel determines the separation performance. For example, the pore size of the gel and its distribution significantly affect the selectivity of SEC, which is usually lower for very large-sized particles.[35] Moreover, interactions between the stationary phase gel and tar-get EMNPs not only affect the EMNPs' original morphology but also lead to a loss in recovery as a result of irreversible adsorption. In contrast, the absence of the stationary phase in the F4 channel results in negligible mechanical or shear stress on the EMNPs caused by the packing materials and a wide choice of aqueous carrier solutions available for use in F4 (e.g., water with or without additives such as surfactants), leading to a high compatibility of F4 with various detectors (e.g., ICPMS). Particularly, the semiper-meable membrane in the F4 separation channel is used to prevent analytes from being lost and remove unwanted components with a size less than the membrane pore size, making it possible to directly analyze EMNPs in complex environmental matrices.

In F4, fractionation of differently sized EMNPs was achieved by applying two right-angled flow streams to the particles. Based on the number of permeable walls envelop-ing semipermeable membranes in the rectangular channel, conventional F4 mainly consists of symmetrical F4 (SF4) and asymmetrical F4 (AF4).[34] The latter variant with a single semipermeable wall achieves better fractionation capability and hence is pres-ently the more commonly used configuration. Another novel variation uses disposable hollow fibers as a channel and is termed as hollow fiber F4 (HF5). Therein, the channel volume and its running costs are decreased, and this configuration is also easy to assemble.[36] Therefore, HF5 is referred to as a disposable F4 technique. To date, AF4 and HF5 have been the most widely used variants of F4 for particle separation and will be highlighted in this review.

In this review, we aim to: (1) summarize the specific advantages of the F4 technique (mainly AF4 and HF5) in the separation of EMNPs; (2) generalize the development of the F4-ICPMS technique; (3) highlight recent advances in the application of AF4-ICPMS and HF5-ICPMS hyphenations for the characterization of EMNPs in the envir-onment; (4) discuss the current perspectives on these two hyphenated techniques for the expansion of applications.

2. Specific advantages of the F4 technique in the separation of EMNPs

F4 instruments generally consist of a constant flow liquid chromatographic pump used for transporting the carrier liquid, an injector, a separation channel, and a detector for recording the elution analytes.[34] A special syringe pump sometimes is used to generate the flow field, which can also be achieved inside the separation channel by the same pump together with switching valves. The separation channels having a rectangular cross-section in SF4 and AF4 or a circular cross-section in HF5 are the core

components of F4 instruments. Sample separation takes place inside the separation channel depending on their hydrodynamic sizes due to the combined action of a laminar flow and an orthogonal flow. Therefore, the accurate flow control system is one of the most important aspects to be considered in the instrumental design. Additionally, the membrane pore size and pore distribution in the separation channel determine the sample recovery as well as separation efficiency.

2.1. Separation of EMNPs in the full particle size range

A striking advantage of the F4 technique over other flow-based separation techniques such as SEC is theoretical application to a wide particle size range (1 nm–100 μm), covering the full size range of EMNPs. In practice, SEC is rarely applied to nanoparticles exceeding a certain size (e.g., 50 nm),[35] which is mainly defined by the SEC stationary phase. For the particles too large to enter pores in the stationary phase, they will be eluted without retention. Therefore, the pore sizes in stationary phase determine the exclusion limit in SEC.[37] The lower limit of the applicability of F4 depends on the exclusion limit of the semipermeable membrane, and the upper limit depends on the separation channel thickness (w).

According to the particle size relative to the diffusion distance, generally two separation modes can be applied in F4, namely normal mode and steric/hyperlayer mode.[34,38] EMNPs can be separated using the normal mode, as their sizes are smaller than 100 nm. Hence, applications of the steric/hyperlayer mode for particles generally larger than 1 μm exceed the scope of this review. In the normal mode, diffusion acts as the opposing force and controls the particle distribution across the channel. The balance between flow field and diffusion enables the particle cloud to reach a characteristic average thickness (l) above the accumulation wall, resulting in an exponential distribution of different thicknesses. The value of l depends on the diffusion coefficient relative to the particle size. The retention parameter (λ) is an important parameter in understanding retention principles of AF4 or HF5. λ is defined as the ratio of l to w, and is related to the measurable experimental parameters of retention ratio (R) (equation 1):[34]

$$R = \frac{t_0}{t_r} \tag{1}$$

where t_0 and t_r correspond to the retention times of the unretained analyte passing through the separation channel and the retained analyte subjected to the flow field, respectively.

The relationship between λ and the physiochemical parameters of the analytes in AF4 can be expressed as:[39]

$$\lambda = \frac{kTV^0}{3\pi\eta V_c w^2 d} \tag{2}$$

where k is Boltzmann's constant, T is the absolute temperature, V^0 is the geometric volume of the separation channel, η is the viscosity of the carrier liquid, V_c is the rate of the cross-flow volume, and d is the hydrodynamic diameter of the analyte. Similarly, the relationship between λ and the physiochemical parameters of the analytes in HF5 can be expressed as:[40]

$$\lambda = \frac{kT}{3\pi\eta Ur_f d} \tag{3}$$

where U is the radial-flow rate at the fiber wall, and r_f is the inner radius of the fiber.

As described above, λ is directly associated with the hydrodynamic diameter of the retained particles (equations 2 and 3) and with the experimentally measured R values (equation 1). Therefore, λ is the link between theoretical and experimental parameters. The relationship between R and λ in HF5 can be written as follows:[41]

$$R = 4\lambda/(1-\lambda) - 12\lambda^2 \tag{4}$$

and

$$R = 4\lambda \tag{5}$$

The retention ratio of HF5 is different from that ($= 6\ \lambda$) of AF4 due to the cylindrical nature of the channel design of HF5.[42] The accuracy of R according to equation 4 is less than 2% for $\lambda < 0.2$, while it is less than 5% for $\lambda < 0.02$ according to equation 5.[41,42] As the experimental R value can be calculated by equation 1, the λ value can be obtained using equations 4 and 5 and further used to calculate the size of the target particles by equations 2 and 3.

According to the retention theory, the retention time in the normal mode of F4 significantly increases with the increase in the size of the target particles, leading to a longer analysis time. Cross-flow programming could present an efficient method to improve the separation of larger nanoparticles that are strongly retained.

2.2. High size-based selectivity

The ability of separation techniques to separate two analytes is evaluated based on the techniques' selectivity. The selectivity of the separation with F4 based on particle size alone is defined as:[43]

$$S_d = \left| \frac{d(\log t_r)}{d(\log d)} \right|$$

High size-based selectivity is another main advantage of F4 compared with other flow-based separation techniques such as SEC. Typically, the S_d value of F4 varies in the range of 0.4–1[40,44] and is generally larger than that of SEC, which is usually smaller than 0.2[45] and decreases significantly for larger-sized NPs. The S_d value of F4 increases when the retention time difference of different-sized particles increases. Furthermore, a high S_d value of F4 indicates that a small change in particle size could lead to a larger change in retention time.

In F4, the size-based selectivity was found to be closely related to the type of membrane, the flow field strength, and other conditions, such as the axial-flow rate. To achieve a better selectivity, it is important to choose a separation membrane with an appropriate pore size or a molecular weight cutoff. In the separation of AgNPs, the selectivity of regenerated cellulose and polyethersulfone membranes with the same pore size were both higher than that of polyvinylidene difluoride membrane.[46,47] This could be due to the fact that the electrostatic repulsion between the negatively charged AgNPs

and the negatively charged polyvinylidene difluoride membrane was lower. The membrane's pore size, expressed as the molar mass cutoff, is usually selected based on the smallest particles in a sample, and an available membrane with a 10-kDa cutoff is most commonly used for the separation of EMNPs. It has been shown that the selectivity could be improved by increasing the cross-flow rate in AF4 or the radial-flow rate in HF5.[41,48] Although the higher axial flow will drive particles located at different equilibrium heights against the fiber wall in a shorter analysis time, its effect on the selectivity of AF4 or HF5 is often examined by controlling the ratio of cross or radial-flow rate and the axial-flow rate.[32,49] In addition, careful optimizations of the properties of the carrier liquid (i.e., composition and pH) and the focusing time may also lead to an improved size-based selectivity.[50–52]

2.3. Characterization of EMNPs in their intact and native state

Although F4 and SEC have similar experimental setups, separation in F4 takes place in an open channel without stationary phase rather than in a column with packing materials, as used for separation in SEC. Specifically, the separation mechanism in F4 is derived from the interaction of the analyte with an external flow field that is applied orthogonally to the separation channel instead of adsorption on the stationary phase.[34] Thus, negligible shear force or mechanical stress is applied to the EMNPs in the samples, enabling the characterization of intact EMNPs, EMNPs with macromolecular coating (i.e., corona structure), and aggregated EMNPs under native conditions. Even under the strong flow field, the risk of EMNP adsorption on the surface of the F4 channel is much lower than that of the SEC column, as the surface area of the F4 membrane is usually less than a thousandth of that of the SEC package material.[53]

In addition, the aqueous solution can be used nearly completely as the carrier liquid of F4 due to the absence of the stationary phase, which is also beneficial for maintaining intact EMNPs and EMNP derivatives under mild separation conditions. In contrast, the use of the buffer solution as the carrier liquid is often required in other separation techniques such as capillary electrophoresis,[54] possibly leading to the aggregation of nanoparticles or loss of their coating structure. Moreover, the versatility of the carrier liquid of F4 makes this method very compatible with commonly used detection methods, such as ultraviolet and visible absorption spectroscopy,[32,55,56] multi-angle light scattering,[57,58] atomic absorption spectroscopy[59], ICPMS[31], etc.

2.4. In-line clean-up of complex matrices

A semipermeable membrane—either the flat membrane in SF4 and AF4 or the cylindrical membrane in HF5—allows cross flow in SF4 and AF4 or radial flow in HF5 to pass through its pores while preventing analyte particles that are larger than the pore size from permeating the membrane.[41] Furthermore, the cross or radial flow carries unwanted species (e.g., ions in the sample) that are smaller than the pore size out of the separation channel during the focusing/relaxation step. After that, the sample composition is effectively simplified and nanoparticles are isolated from complex matrices, which is favorable for the accurate analysis by on-line detectors (e.g., lower background
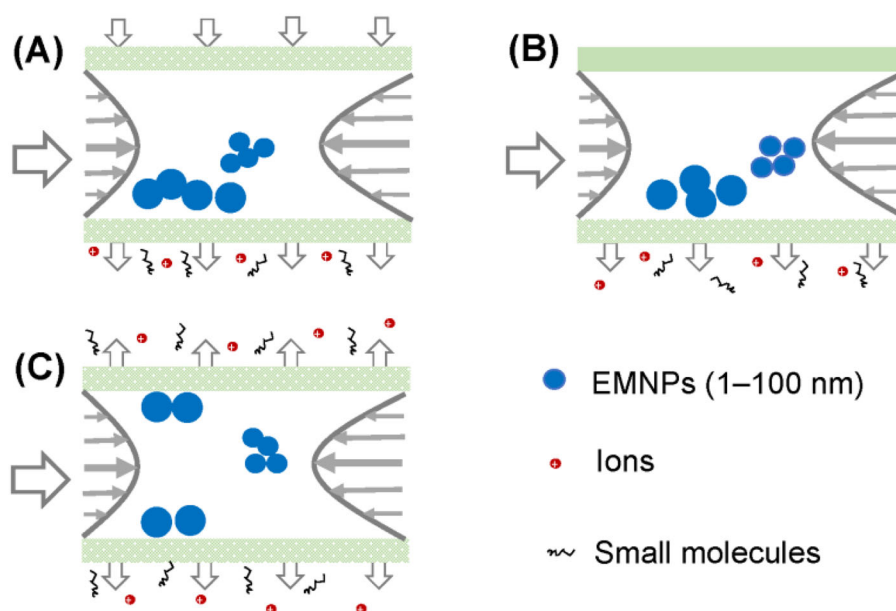
Figure 1. Distributions of two-sized EMNPs over the parabolic flow profile during the focusing/relaxation step of SF4 (A), AF4 (B), and HF5 (C). The unwanted species (e.g., ions and small molecules) are filtered out of the separation channel.

noise) in the elution step. Therefore, in addition to its separation function, the semipermeable membrane in the F4 channel has the function of an in-line sample clean-up.

During the focusing/relaxation step in HF5, sample matrix components can be collected off-line or on-line to further detect the newly formed species. For example, Ag(I) ions coexisting with AgNPs were identified by atomic absorption spectroscopy after off-line collection.[58] Using a mini-column packed with Amberlite IR120 resin at the radial outlet of HF5, we successfully separated free Ag(I) or weak Ag(I) complexes from strong Ag(I) complexes and tiny AgNPs ($<$ 2 nm), which were further discriminated and determined by the oxidation of tiny AgNPs to free Ag(I) in a second run. Applying this strategy, the developed on-line HF5 and mini-column-concentration with ICPMS achieved the full spectrum of separation, identification, and quantification of two Ag(I) species (including free Ag(I) or weak and strong Ag(I) complexes) and five different-sized AgNPs (1.4, 10, 20, 40, and 60 nm).[32] In contrast, few studies have been reported on the on-line collection during the focusing/relaxation step in AF4, which is partly due to the fact that the cross-flow rate is too high for the sampling system to directly enter the following detectors.

3. General development of F4-ICPMS for EMNP characterization

After transport of EMNPs into the thin ribbon-like channel (SF4 and AF4) or hollow fiber channel (HF5) by a carrier liquid, particles of different sizes adopted a steady-state distribution during the focusing/relaxation step, as shown in Figure 1. After that, the particles are delivered to the outlet of the channel by the flow of the carrier liquid with a parabolic flow profile in the elution step. Then, the eluted particles reach the ICPMS

detector sequentially according to their sizes. Therefore, the retention time is strictly dependent on the particle size. Thus, ICPMS detection provides information about the retention time, which allows the calculation of the size and size distribution of separated particles and the analysis of their elemental composition for identification and quantification.

ICPMS was first coupled with conventional F4 (i.e., SF4 and AF4) to obtain information on the size and concentration of metal-containing colloidal particles. In an earlier study, on-line coupling of SF4 with ICPMS was used to determine the sizes of colloidal particles and the distributions of 28 elements in natural waters.[60] Later, an on-line AF4-ICPMS coupling system was developed to quantify trace elements associated with colloids in soil leachates.[61] The accuracy of the determination of six chosen trace elements was validated through an off-line quantification procedure using fraction collection and total elemental analysis by ICPMS. Earlier studies demonstrated the great potential of the F4-ICPMS coupling system in the identification and quantification of EMNPs. EMNP characterization using the F4-ICPMS technique was first reported for AuNPs,[30] mainly due to their ease of preparation, good stability, and wide range of applications. The limit of detection of AuNPs in the size range of 10–60 nm varied between 0.02 and 0.4 ng Au, which was directly proportional to the nanoparticle diameter. Furthermore, the developed coupling system was successful in analyzing and recovering AuNPs in the livers of rats in the range of 86–123%. Due to the continuous use and wide range of applications of AgNP-based products, the characterization of AgNPs in environmental and biological matrices using AF4-ICPMS has been extensively studied.[56,62,63] Very recently, the F4-ICPMS-based method has also been extended for the characterization of PtNPs,[64] which are EMNPs that are frequently used in the automotive sector, electrochemistry, and biomedical applications.[65]

Generally, the large volume of the rectangular channel in AF4 is readily to dilute the sample. Moreover, due to the very high cross-flow rates (e.g., 1.5 mL/min), a split system between the channel outlet and the nebulizer was often used to withdraw a fraction of the outlet flow for detection. In contrast, the outlet flow rate of the HF5 channel is usually very low, which makes flow splitting not required. Although studies have shown that the AF4-ICPMS system is more mature and more versatile than the HF5-ICPMS system due to the more commercial availability of AF4, the unique features of HF5, such as the disposable hollow fiber channel, easy installation, and lower flow rates, deserve more attention.

4. Recent advances in the application of the F4-ICPMS system in the characterization of EMNPs in the environment

With the widespread use of EMNPs and their products in the industrial production and daily life, EMNPs inevitably enter the environment. As shown in Figure 2, EMNPs can enter waste water treatment plants (WWTPs), natural water bodies, soil/sediment, organisms, or the atmosphere (not shown). In their biogeochemical cycling, EMNPs undergo various physical and chemical transformations. Given the aforementioned specific advantages of F4, F4-ICPMS systems open up new avenues for the characterization of EMNPs in environmental samples and tracking their transformations in the
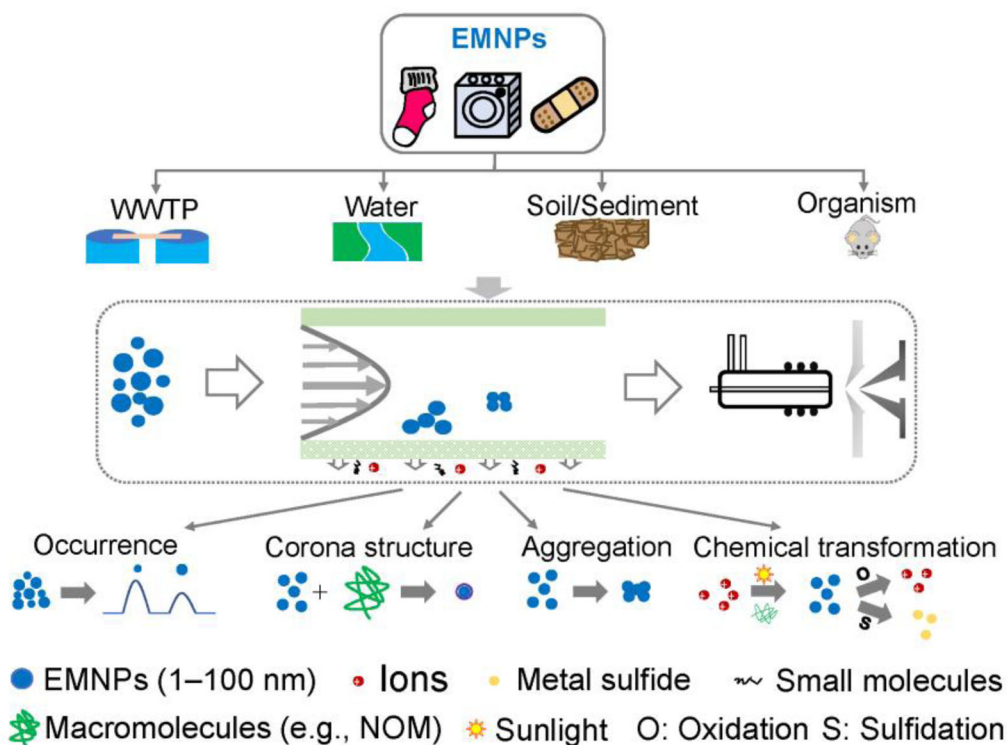
Figure 2. Recent advances in characterization of EMNPs released into the various environmental media using the F4-ICPMS technique.

environment. In the following, we reviewed the recent advances in these fields, including the estimation of EMNP occurrence in various environmental samples, characterization of corona-coated EMNPs, tracking of the aggregation of EMNPs in the environment, and speciation analysis of EMNPs and their products in their main chemical transformations.

4.1. Estimation of the occurrence of EMNPs in various environmental media

Size, composition, and concentration are the most important characteristics of EMNPs in environmental media. It has been experimentally shown that the environmental fate, transport, and risk of EMNPs are closely associated with these characteristics,[12,66] inspiring the development of various methods for the comprehensive characterization of EMNPs. F4-ICPMS-based methods can achieve the full range of accurate separation, identification, and quantification of EMNPs, making them the most promising candidates for the characterization of EMNPs in various environmental matrices.

Extensive applications of EMNPs inevitably lead to the release of EMNPs into the environment, and particularly aqueous environment, through the direct release as industrial discharges, effluents from residential households, or disposed effluents from WWTPs.[67,68] Natural surface water matrices are relatively simple, and the in-line

clean-up ability of F4 can effectively further reduce matrix-induced interferences from metal ions, low molecular weight molecules, small-sized particles, *etc*. Therefore, F4-ICPMS can be directly used to obtain information about size and concentration of EMNPs in natural surface water samples after very simple pretreatments, such as filtration.[32] WWTPs have been reported to be the main sink as well as the point sources of EMNPs. An on-line AF4-ICPMS system was used for the determination of the size and concentration of AgNPs in untreated influent of WWTPs, showing that the mean size and concentration of AgNPs in the influent were 9.3 nm and 1.90 ng/mL, respectively.[56] These results clearly demonstrated the robustness of the AF4-ICPMS system for the characterization of trace amount of EMNPs in complex aqueous matrices.

Sediments and soil systems are usually considered to be the ultimate sinks of EMNPs in the natural environment.[69] Simulation models have estimated that the highest proportion of EMNPs in the environment is present in sediments and soil,[70] whose matrices are much more complex than those of water samples. Therefore, it is necessary to effectively extract EMNPs from the solid matrix into a stable liquid suspension prior to F4-ICPMS analysis. Moreover, EMNPs displayed a tendency for surface adsorption on clay minerals, especially colloids. Hence, only few studies have focused on the characterization of EMNPs in sediments and soil, arguing the overestimation of the EMNPs' original size due to the unavoidable interaction between coexisting components, such as colloidal clay minerals.[71] Sodium pyrophosphate has exhibited excellent ability in the extraction of relative stable nanomaterials such as TiO_2 and CeO_2 by promoting their release from microaggregates in soil,[72] but the universality in extracting reactive EMNPs remains unexploited. Therefore, it is highly urgent to develop efficient sample pretreatments to isolate EMNPs that are present in sediments and soil, which would greatly improve the applicability of the F4-ICPMS method for the accurate characterization of EMNPs in such complex matrices.

The presence of EMNPs in organisms can be ascribed to many sources, such as their deliberate use as medicine, uptake by organisms, and transfer in food chains.[73–75] In the field of environmental nanotoxicology, AF4-ICPMS has also been used for the characterization of EMNPs in biological matrices. In a milestone study, AF4-ICPMS was successfully used for the identification and quantification of intact AuNPs in rate livers after dissolution with tetramethylammonium hydroxide.[30] In comparative experiments on the dissolution medium for EMNP-exposed *D. magna*, AF4-ICPMS showed comparable results of both tetramethylammonium hydroxide and trypsin for medium-sized (50 nm) EMNPs, including AgNPs, AuNPs, and PtNPs, but trypsin seems advantageous to maintain the original small-sized (5 nm) particles.[76] This finding highlights the importance of the dissolution medium used for extracting EMNPs in organisms prior to AF4-ICPMS analysis. In addition, a relevant human lung cell line (THP-1) was used to study the *in vitro* uptake of medium-sized AgNPs (50–75 nm). Results of AF4-ICPMS clearly showed that the AgNP size varied with time, demonstrating the high dynamics of AgNPs during cell exposure. Moreover, the uptake of AgNPs was found to be dependent on the composition of the medium and the particle size.[77] These findings demonstrated that the AF4-ICPMS system would be a promising candidate for characterization of EMNPs *in vitro* and *in vivo* studies focusing on their toxicity and biodistribution.

4.2. Characterization of corona-coated EMNPs

After the uptake of EMNPs by organisms, they will get into contact with the abundant biomolecules, such as proteins and lipids, forming a bio-corona structure of macromolecules around the EMNP surface.[78,79] In environmental nanotoxicology, characterization of the bio-corona structure will provide a deeper insight into the potential risk of EMNPs. Recently, it has been reported that EMNPs released into the aqueous environment tender to interact with macromolecules, such as natural organic matters (NOM), to form an eco-corona structure, dominating the fate and transport of EMNPs.[80] The thickness of the intact corona structures varied from several nanometers to sub-micrometers. For an accurate characterization of such EMNPs, F4 is a suitable method due to its applicability in a wide particle size range with high size-based selectivity but operation under gentle separation conditions (e.g., negligible mechanical or shear stress due to the absence of the stationary phase).

Although there have been decades of research on bio-corona formation around EMNPs, studies on the characterization of bio-coronas using the F4-ICPMS system just emerged recently. An early study on the association of different-sized AgNPs (i.e., sizes of 2.6, 10, and 26 nm) with proteins showed that the amounts of three common proteins (bovine serum albumin, globulin, and fibrinogen) adsorbed on the AgNP surface was positively correlated with the incubation time and concentration of AgNPs.[81] In stoichiometric binding experiments, the ratio of bovine serum albumin to AgNPs was calculated to be approximately $1:5 \times 10^{-7}$. These findings demonstrated a potential application of F4-ICPMS in quantitatively tracking the formation process of the bio-corona structure. In the evaluation of the stability of AuNPs in DMEM (10% FBS), as a commonly used cell culture medium, AF4-ICPMS demonstrated a visible increase in the AuNP size, which can be probably ascribed to the bio-corona formation. These results stress the necessity to consider the changes of primary EMNPs in culture medium before an *in vitro* toxicity test.[82] Moreover, the type of protein plays a key role in bio-corona formation and the resulting stability of EMNPs. Taking the two mammalian metalloproteins of intracellular metallothionein 1 (MT1) and plasmatic ceruloplasmin (Cp) as examples, the significant difference in their protein-corona dynamics could be detected by AF4-ICPMS. After interaction of unstructured MT1 with AgNPs, MT1 rapidly surrounded the AgNPs with a transient corona, which was rapidly transformed into a larger envelope. Interaction of well-structured and globular Cp with AgNPs resulted in the formation of a more stable bio-corona layer around the AgNPs. Nevertheless, both types of protein coronas promoted the dissolution of AgNPs, which was closely related to the properties of the proteins, such as their geometry and accessibility to metal binding sites.[83] These findings highlight the fact that the type of protein has a great influence on the bio-corona formation and EMNP stability in biofluids, which will govern the fate of EMNPs *in-vivo*.

Although some unexpected results on bio-coronas have been achieved by F4-ICPMS, the characterization of eco-coronas by this powerful technique is still in its infancy and needs further development. Only a decade ago, coating of NOM molecules onto the surface of AgNPs was proven by AF4-ICPMS. The obtained fractograms showed a slight increase in the elution time of AgNPs in the NOM-rich solution, indicating an increase in the AgNP particle size, which was ascribed to eco-corona formation.[84] Recently, we

reported the quantitative characterization of an eco-corona by HF5-ICPMS and studied the effect of the NOM concentration on the thickness of the eco-corona in detail.[85] The size of AgNPs was calculated from their retention time obtained from factograms, revealing that the AgNP size increased from 8.8 ± 0.39 nm to 23.2 ± 0.70 nm with the increase of the NOM concentration from 10 to 100 mg/L dissolved organic matter. The composition of the corona structure was further analyzed from scanning transmission electron microscopy images and energy dispersive spectroscopy mapping results, indicating that both the C- and O-enriched areas overlapped significantly with the Ag-enriched area. The eco-corona around the EMNPs significantly affected their surface chemistry and behavior in environmental systems, especially their aggregation behavior. Moreover, thermodynamic and kinetics information on the eco-corona formation process will contribute to deep understandings of dynamic interactions between EMNPs and with other naturally occurring macromolecules as well as NPs in natural environments.

4.3. Tracking of EMNP aggregation in the environment

Aggregation is regarded as an important physical transformation of EMNPs in the environment. The aggregation process increases the effective particle size and reduces the surface area to volume ratio, thereby affects the EMNPs' reactivity, transport, and uptake by living organisms.[12,86] The aggregation of EMNPs can be divided into two categories: homoaggregation between the same type of EMNPs and heteroaggregation between EMNPs and other coexisting particles.[87] Dynamic light scattering is the most commonly used technique to study aggregation processes. However, it has some disadvantages such as low selectivity and low accuracy in the analysis of large particles, which greatly limits its use in the characterization of heteroaggregated EMNPs.[88] Although the significant increase in the size of aggregated EMNPs could be analyzed by SEC, the reduced stability of aggregated EMNPs may lead to problems of irreversible sample adsorption and carryover between runs. The absence of the stationary phase makes F4 ideally suited for the characterization of aggregated EMNPs in native and intact forms.

Currently, a great deal of studies on EMNP aggregation under controlled laboratory conditions focused on homoaggregation.[64,89,90] These studies focused on predicting the fate of EMNPs in relatively simple matrices, such as natural surface waters, and experimental results followed the Derjaguin-Landau-Verwey-Overbeek theory. Early studies mainly focused on the effects of solution chemistry (e.g., pH, type of salt, ionic strength, NOM) on the aggregation of EMNPs.[91] AF4-ICPMS provided direct results on the size change of aggregated EMNPs with increasing destabilization due to the changed experimental conditions, e.g., the increased ionic strength.[84] A comparative study on the aggregation behavior of 60 nm AgNPs in various aqueous matrices showed that the particle size did not change significantly after incubation for two days in deionized water, while AgNPs could no longer be detected after the same incubation time in artificial sea water, confirming the strong destabilizing effect of high ionic strengths.[92] The volume of the HF5 channel is relatively smaller than that of the AF4 or SF4 channel, resulting in less dilution of EMNPs in HF5 separation and a more

sensitive detection of EMNPs at low concentrations. Using HF5-ICPMS, we studied the aggregation of AgNPs at environmentally relevant concentrations in aqueous conditions.[85] Interestingly, we found that the attachment efficiency, standing for the attachment probability of two particles, of AgNPs at a concentration of 10 ng/mL in the presence of various concentrations of Na(I) ions and Ca(II) ions was much higher than those reported for AgNPs at relatively high concentrations (e.g., concentrations at the µg/mL level). These results demonstrated the sensitivity of HF5-ICPMS in studying the aggregation of EMNPs at a low concentration and highlighted the necessity of studying EMNP aggregation at environmentally relevant concentrations. The effect of NOM on EMNP aggregation is quite controversial. On the one hand, the eco-corona could inhibit aggregation by steric repulsion or/and electrostatic repulsion;[93] on the other hand, the bridging effect could lead to the destabilizing effect of NOM.[94] Whether stabilization or destabilization dominated was found to be closely related to the type of NOM and the NOM concentration.[95] Besides solution chemistry, other environmental factors, such as sunlight, also had a substantial influence on the aggregation of EMNPs. F4-ICPMS fractograms showed that, in the presence of sunlight, smaller sized AgNPs (e.g., 20 nm AgNPs) transformed into multifaceted particles, whereas the shapes of larger particles (e.g., 60 and 80 nm AgNPs) were mainly modified by aggregation.[96]

Real environmental systems, especially soil and sediment, contain abundant amounts of natural particles, whose concentrations are usually much higher than that of EMNPs. Therefore, heteroaggregation occurs most likely in these complex matrix systems.[97] Nevertheless, there are relatively few studies on EMNP heteroaggregation processes, partially due to the lack of characterization methods for heteroaggregated EMNPs in the intact state. Recently, AF4-ICPMS has been used to study EMNP heteroaggregation processes. In studying the stability of AuNPs in colloidal soil extract containing natural nanoparticles, the differentiation of heteroaggregation and homoaggregation of AuNPs was performed by AF4-ICPMS through analyzing the size and components of aggregated AuNPs.[69] In addition to the need for optimizing the operating parameters of AF4 in the separation of different-sized aggregated AuNPs, this work highlighted the importance of extracting the aggregated AuNPs from the soil matrix into stable liquid suspensions. In addition, it has been found that the coating type of AuNPs greatly affects heteroaggregation. Compared with citrate-coated AgNPs, PVP-coated AgNPs could not be determined accurately, mainly due to the fact that their stronger interactions with colloidal clay minerals made their isolation by the common wet extraction procedure difficult.[71] Similar results were obtained for AuNPs with various coatings. AF4-ICPMS results demonstrated that Au is co-eluted with other elements such as Al, Fe, and Mn, indicating the occurrence of heteroaggregation between AuNP and the soil colloids. These results also showed that NOM could replace the coating of AuNPs and be adsorbed on the mineral particles. With this, the influences on the native surface chemistry of EMNPs and functional coatings become difficult to predict. Furthermore, a kinetic study showed that such an attachment controlled by heteroaggregation is a rather fast process (e.g., over 80% AuNPs aggregated after 2 h).[69] These findings strongly confirmed the limitation of the long-range transport of original EMNPs in sediments and soils.

4.4. Speciation analysis of EMNPs and their products in main chemical transformations in natural systems

EMNPs exhibit a high percentage of metal atoms on their large specific surface area, leading to their high reactivity in natural systems. Therefore, various chemical transformations in natural systems, including redox reactions and sulfidation between EMNPs and their derivatives (e.g., metal ions, metal sulfide, *etc*.), ultimately influence the behavior, fate, and risk of EMNPs.[12] For example, Ag(I) ions were found to be more toxic than AgNPs and silver sulfide, so the oxidation of AgNPs into Ag(I) leads to higher toxicity, while the sulfidation of Ag(I) from AgNPs significantly reduces the toxicity.[98] Understanding and predicting these main chemical transformations requires a reliable method for the simultaneous determination of EMNPs and their products. As a rapidly emerging technique for the characterization of EMNPs, F4-ICPMS fulfills all these requirements and is a suitable method for this purpose.

Natural systems are mostly oxidizing environments, so the oxidation of EMNPs to release the corresponding metal ions is one of the most important steps in their chemical transformation in the environment. In studying the oxidation of AgNPs in littoral lake mesocosms, the concentration of AgNPs gradually decreased over time, indicating the oxidation of AgNPs. Moreover, the peak early eluted before that of AgNPs in AF4-ICPMS was reported to stem from the formation of a complex between Ag(I) and NOM.[99] Under sunlight irradiation, NOM could generate abundant reactive oxygen species, resulting in the reduction of EMNPs.[100] We employed the HF5-ICPMS-based coupling system to compare the transformation of Ag(I) at two different concentrations (33.97 µg/mL and 33.97 ng/mL) into AgNPs. Surprisingly, Ag(I) ions were co-eluted with tiny AgNPs in the focusing/relaxation step for an Ag(I) concentration of 33.97 µg/mL, while only large-sized AgNPs were observed for an Ag(I) concentration of 33.97 ng/mL.[85] These findings stressed the necessity of studying the chemical transformations of Ag(I) at environmentally relevant concentrations.

Most noble metals have a strong affinity to sulfur-containing compounds or inorganic sulfur, which promotes the release of metal ions from EMNPs or the insoluble metal-sulfide shell around the particles.[101] Therefore, the sulfidation of EMNPs is another important process that needs to be carefully considered. Taking tripeptide glutathione as a model of sulfur-containing compounds, AF4-ICPMS was used to study the sulfidation of PVP-protected AgNPs.[102] AF4 achieved the separation of a series of newly formed compounds and materials, such as Ag(I), nanoclusters, and nanoparticles, which were quantitatively analyzed by ICPMS. Similarly, mass preservation by PVP-AgNP populations in sulfide-containing simulated water was verified by the hyphenated AF4-ICPMS method.[103] In AgNPs sulfidation experiments, soluble Ag(I) ions including their complexes with sulfur-containing compounds and AgNPs or Ag_2S NPs smaller than the size detection limit of SP-ICPMS are inevitably produced, posing a great analytical challenge for SP-ICPMS, while AF4-ICPMS has shown great potential for charactering the original AgNPs as well as their products during distribution. These findings suggest that hyphenated AF4 provides an in situ method for monitoring the changes of EMNPs in the sulfidation process. HF5-ICPMS was used to simultaneously record the S and Ag signals in a spiked sample from an influent of a local WWTP, and the new thiol-complexed Ag(I) rather than silver sulfide was identified and quantified,

demonstrating the robustness and sensitivity of the HF5-ICPMS method in studying inter-transformations between Ag(I) and AgNPs at environmentally relevant concentrations in domestic wastewater.[85]

5. Conclusions and future perspectives

In this review, we provided an updated summary of hyphenated systems based on F4-ICPMS for the characterization of EMNPs in the environment. These hyphenated systems are indispensable for a deep understanding of the environmental fate and potential risk of EMNPs. Although several advances have been made in the past decade, the research on F4-ICPMS is still in its infancy, and much room still remains for the improvement in performance and application in the characterization of EMNPs.

Several current perspectives on the application of F4-ICPMS for the characterization of EMNPs have been proposed, as discussed in the following.

Firstly, natural, incidental, and engineered EMNPs often coexist in the natural environment, and their sizes, compositions, and concentrations cannot be accurately predicted to date. Specific advantages of F4-ICPMS, such as the applicability to a wide range of particle sizes and high size-based selectivity and sensitivity, make F4-ICPMS a potential tool for the separation, identification, and quantification of these types of EMNPs based on their size difference, size distribution, and composition to provide insight into the source tracing of EMNPs in the natural environment.

Secondly, similar to NOM in the natural environment, extracellular polymeric substances are also ubiquitous in various environmental matrices and play a notable role in the fate and transport of EMNPs. The changes in the structure and chemical properties of EMNPs due to their interactions with different NOM and/or extracellular polymeric substances can be explained by introducing other characterization methods (e.g., Fourier transform ion cyclotron resonance mass spectrometry) to complement the F4-ICPMS coupling system.

Thirdly, the differentiation of EMNPs and their coexisting derivatives, such as their corresponding ions, free ions, and complexes of the corresponding ions, still poses big challenges in real biological matrices in the field of environmental nanotoxicology. Hence, the toxic effects of EMNPs are still not conclusive. EMNPs can be directly characterized in the elution step of AF4-ICPMS, but the characterization of their derivatives by off-line coupling methods is a more feasible strategy.

Fourthly, laboratory experiments on the transformation or uptake of EMNPs in detectable concentrations cannot sufficiently represent real scenarios. Therefore, further improvements in the performance of F4-ICPMS are required. For example, an improvement in sensitivity by injecting large volumes (e.g., 50 mL) may be an effective approach to elucidate various physical and chemical transformations and the intake of EMNPs at ultra-trace levels, which will uncover their fate and behavior during the aging processes or long-term exposure studies.

Last but not the least, intensive studies have demonstrated the feasibility of F4-ICPMS hyphenated systems (especially AF4-ICPMS), but no hyphenated systems are commercially available yet. Action plans to enhance the commercialization of these on-

line coupling systems would favor the standardization of identification and characterization protocols for comparable measurements and reliable risk assessments.

ORCID

Yongguang Yin (iD) http://orcid.org/0000-0001-9392-6256
Baoshan Xing (iD) http://orcid.org/0000-0003-2028-1295

References

1. Son, D.; Bao, Z. A. Nanomaterials in Skin-Inspired Electronics: Toward Soft and Robust Skin-Like Electronic Nanosystems. *ACS Nano* 2018, *12*, 11731–11739. doi:10.1021/acsnano.8b07738
2. Peters, R. J. B.; Bouwmeester, H.; Gottardo, S.; Amenta, V.; Arena, M.; Brandhoff, P.; Marvin, H. J. P.; Mech, A.; Moniz, F. B.; Pesudo, L. Q.; et al. Nanomaterials for Products and Application in Agriculture, Feed and Food. *Trends Food Sci. Technol.* 2016, *54*, 155–164. doi:10.1016/j.tifs.2016.06.008
3. Mauter, M. S.; Elimelech, M. Environmental Applications of Carbon-Based Nanomaterials. *Environ. Sci. Technol.* 2008, *42*, 5843–5859. doi:10.1021/es8006904
4. Barreto, J. A.; O'Malley, W.; Kubeil, M.; Graham, B.; Stephan, H.; Spiccia, L. Nanomaterials: Applications in Cancer Imaging and Therapy. *Adv. Mater.* 2011, *23*, H18–H40. doi:10.1002/adma.201100140
5. Wagner, S.; Gondikas, A.; Neubauer, E.; Hofmann, T.; von der Kammer, F. Spot the Difference: Engineered and Natural Nanoparticles in the Environment — Release, Behavior, and Fate. *Angew. Chem. Int. Ed.* 2014, *53*, 12398–12419.
6. Liu, L. C.; Corma, A. Metal Catalysts for Heterogeneous Catalysis: From Single Atoms to Nanoclusters and Nanoparticles. *Chem. Rev.* 2018, *118*, 4981–5079. doi:10.1021/acs.chemrev.7b00776
7. Pandey, R. K.; Chen, L.; Teraji, S.; Nakanishi, H.; Soh, S. Direct Deposition of Metal Nanoparticles on Graphite for Electrochemical Energy Conversion and Storage. *ACS Appl. Mater. Interfaces* 2019, *11*, 36525–36534. doi:10.1021/acsami.9b09273
8. Kim, K. S.; Kim, J. H.; Yoo, S. I.; Sohn, B. H. Fluorescence Resonance Energy Transfer within Diblock Copolymer Micelles in the Proximity of Metal Nanoparticles. *Macromol. Res.* 2019, *27*, 905–910. doi:10.1007/s13233-019-7127-z
9. Rai, M.; Yadav, A.; Gade, A. Silver Nanoparticles as a New Generation of Antimicrobials. *Biotechnol. Adv.* 2009, *27*, 76–83. doi:10.1016/j.biotechadv.2008.09.002
10. Slavin, Y. N.; Asnis, J.; Hafeli, U. O.; Bach, H. Metal Nanoparticles: Understanding the Mechanisms behind Antibacterial Activity. *J. Nanobiotechnol.* 2017, *15*, 65.
11. Liu, S. J.; Xia, T. Continued Efforts on Nanomaterial-Environmental Health and Safety is Critical to Maintain Sustainable Growth of Nanoindustry. *Small* 2020, *16*, 2000603. doi:10.1002/smll.202000603

12. Lowry, G. V.; Gregory, K. B.; Apte, S. C.; Lead, J. R. Transformations of Nanomaterials in the Environment. *Environ. Sci. Technol.* 2012, *46*, 6893–6899. doi:10.1021/es300839e

13. Levard, C.; Hotze, E. M.; Lowry, G. V.; Brown, G. E. Environmental Transformations of Silver Nanoparticles: Impact on Stability and Toxicity. *Environ. Sci. Technol.* 2012, *46*, 6900–6914. [Database] doi:10.1021/es2037405

14. Ju-Nam, Y.; Lead, J. R. Manufactured Nanoparticles: An Overview of Their Chemistry, Interactions and Potential Environmental Implications. *Sci. Total Environ.* 2008, *400*, 396–414. doi:10.1016/j.scitotenv.2008.06.042

15. Deng, R.; Lin, D. H.; Zhu, L. Z.; Majumdar, S.; White, J. C.; Gardea-Torresdey, J. L.; Xing, B. S. Nanoparticle Interactions with Co-Existing Contaminants: Joint Toxicity, Bioaccumulation and Risk. *Nanotoxicology* 2017, *11*, 591–612. doi:10.1080/17435390.2017.1343404

16. Guo, X. R.; Yin, Y. G.; Tan, Z. Q.; Liu, J. F.; Jiang, G. B. Catalytic Oxidation of Arsenic in Water by Silver Nanoparticles. *Acta Chimica Sinica* 2018, *76*, 387–392. doi:10.6023/A18020067

17. Bilberg, K.; Malte, H.; Wang, T.; Baatrup, E. Silver Nanoparticles and Silver Nitrate Cause Respiratory Stress in Eurasian Perch (*Perca Fluviatilis*). *Aquat. Toxicol.* 2010, *96*, 159–165. [Database] doi:10.1016/j.aquatox.2009.10.019

18. Brun, N. R.; Koch, B. E. V.; Varela, M.; Peijnenburg, W. J. G. M.; Spaink, H. P.; Vijver, M. G. Nanoparticles Induce Dermal and Intestinal Innate Immune System Responses in Zebrafish Embryos. *Environ. Sci: Nano* 2018, *5*, 904–916. doi:10.1039/C8EN00002F

19. Vali, S.; Mohammadi, G.; Tavabe, K. R.; Moghadas, F.; Naserabad, S. S. The Effects of Silver Nanoparticles (Ag-NPs) Sublethal Concentrations on Common Carp (*Cyprinus Carpio*): Bioaccumulation, Hematology, Serum Biochemistry and Immunology, Antioxidant Enzymes, and Skin Mucosal Responses. *Ecotoxicol. Environ. Saf.* 2020, *194*, 110353. doi:10.1016/j.ecoenv.2020.110353

20. Schrand, A. M.; Rahman, M. F.; Hussain, S. M.; Schlager, J. J.; Smith, D. A.; Ali, S. F. Metal-Based Nanoparticles and Their Toxicity Assessment. *WIREs Nanomed. Nanobiotechnol.* 2010, *2*, 544–568. doi:10.1002/wnan.103

21. Liu, W.; Wu, Y. A.; Wang, C.; Li, H. C.; Wang, T.; Liao, C. Y.; Cui, L.; Zhou, Q. F.; Yan, B.; Jiang, G. B. Impact of Silver Nanoparticles on Human Cells: Effect of Particle Size. *Nanotoxicology* 2010, *4*, 319–330. doi:10.3109/17435390.2010.483745

22. Meermann, B.; Nischwitz, V. ICP-MS for the Analysis at the Nanoscale — a Tutorial Review. *J. Anal. At. Spectrom.* 2018, *33*, 1432–1468. doi:10.1039/C8JA00037A

23. He, M.; Chen, B. B.; Wang, H.; Hu, B. Microfluidic Chip-Inductively Coupled Plasma Mass Spectrometry for Trace Elements and Their Species Analysis in Cells. *Appl. Spectrosc. Rev.* 2019, *54*, 250–263. doi:10.1080/05704928.2019.1565864

24. Wang, X. Y.; Yin, X. B.; Zeng, Z. G.; Chen, S. Multi-Element Analysis of Ferromanganese Nodules and Crusts by Inductively Coupled Plasma Mass Spectrometry. *At. spectrosc.* 2019, *40*, 153–160. doi:10.46770/AS.2019.05.001

25. Laborda, F.; Bolea, E.; Jimenez-Lamana, J. Single Particle Inductively Coupled Plasma Mass Spectrometry for the Analysis of Inorganic Engineered Nanoparticles in Environmental Samples. *Trends Environ. Anal. Chem.* 2016, *9*, 15–23. doi:10.1016/j.teac.2016.02.001

26. Liu, L. H.; Yin, Y. G.; Hu, L. G.; He, B.; Shi, J. B.; Jiang, G. B. Revisiting the Forms of Trace Elements in Biogeochemical Cycling: Analytical Needs and Challenges. *TrAC, Trends Anal. Chem.* 2020, *129*, 115953. doi:10.1016/j.trac.2020.115953

27. Flores, K.; Turley, R. S.; Valdes, C.; Ye, Y. Q.; Cantu, J.; Hernandez-Viezcas, J. A.; Parsons, J. G.; Gardea-Torresdey, J. L. Environmental Applications and Recent Innovations in Single Particle Inductively Coupled Plasma Mass Spectrometry (SP-ICP-MS). *Appl. Spectrosc. Rev* 2021, *56*, 1–26. doi:10.1080/05704928.2019.1694937

28. Zhou, X. X.; Liu, R.; Liu, J. F. Rapid Chromatographic Separation of Dissoluble Ag(I) and Silver-Containing Nanoparticles of 1-100 Nanometer in Antibacterial Products and

Environmental Waters. *Environ. Sci. Technol.* 2014, *48*, 14516–14524. doi:10.1021/es504088e

29. Pitkanen, L.; Bustos, A. R. M.; Murphy, K. E.; Winchester, M. R.; Striegel, A. M. Quantitative Characterization of Gold Nanoparticles by Size-Exclusion and Hydrodynamic Chromatography, Coupled to Inductively Coupled Plasma Mass Spectrometry and Quasi-Elastic Light Scattering. *J. Chromatogr. A* 2017, *1511*, 59–67. doi:10.1016/j.chroma.2017.06.064

30. Schmidt, B.; Loeschner, K.; Hadrup, N.; Mortensen, A.; Sloth, J. J.; Koch, C. B.; Larsen, E. H. Quantitative Characterization of Gold Nanoparticles by Field-Flow Fractionation Coupled on-Line with Light Scattering Detection and Inductively Coupled Plasma Mass Spectrometry. *Anal. Chem.* 2011, *83*, 2461–2468. doi:10.1021/ac102545e

31. Pornwilard, M. M.; Siripinyanond, A. Field-Flow Fractionation with Inductively Coupled Plasma Mass Spectrometry: Past, Present, and Future. *J. Anal. At. Spectrom.* 2014, *29*, 1739–1752.

32. Tan, Z. Q.; Liu, J. F.; Guo, X. R.; Yin, Y. G.; Byeon, S. K.; Moon, M. H.; Jiang, G. B. Toward Full Spectrum Speciation of Silver Nanoparticles and Ionic Silver by on-Line Coupling of Hollow Fiber Flow Field-Flow Fractionation and Minicolumn Concentration with Multiple Detectors. *Anal. Chem.* 2015, *87*, 8441–8447. doi:10.1021/acs.analchem.5b01827

33. Giddings, J. C. Field-Flow Fractionation: Analysis of Macromolecular, Colloidal, and Particulate Materials. *Science* 1993, *260*, 1456–1465. doi:10.1126/science.8502990

34. Wahlund, K. G. Flow Field-Flow Fractionation: Critical Overview. *J. Chromatogr. A* 2013, *1287*, 97–112. doi:10.1016/j.chroma.2013.02.028

35. Pitkänen, L.; Striegel, A. M. Size-Exclusion Chromatography of Metal Nanoparticles and Quantum Dots. *TrAC, Trends Anal. Chem.* 2016, *80*, 311–320. doi:10.1016/j.trac.2015.06.013

36. Joensson, J. A.; Carlshaf, A. Flow Field Flow Fractionation in Hollow Cylindrical Fibers. *Anal. Chem.* 1989, *61*, 11–18. doi:10.1021/ac00176a004

37. Kostanski, L. K.; Keller, D. M.; Hamielec, A. E. Size-Exclusion Chromatography—A Review of Calibration Methodologies. *J Biochem. Biophys. Methods* 2004, *58*, 159–186. doi:10.1016/j.jbbm.2003.10.001

38. Min, B. R.; Kim, S. J.; Ahn, K. H.; Moon, M. H. Hyperlayer Separation in Hollow Fiber Flow Field-Flow Fractionation: Effect of Membrane Materials on Resolution and Selectivity. *J. Chromatogr. A.* 2002, *950*, 175–182. doi:10.1016/S0021-9673(02)00029-8

39. Baalousha, M.; Stolpe, B.; Lead, J. R. Flow Field-Flow Fractionation for the Analysis and Characterization of Natural Colloids and Manufactured Nanoparticles in Environmental Systems: A Critical Review. *J. Chromatogr. A* 2011, *1218*, 4078–4103. doi:10.1016/j.chroma.2011.04.063

40. Moon, M. H.; Lee, K. H.; Min, B. R. Effect of Temperature on Particle Separation in Hollow Fiber Flow Field-Flow Fractionation. *J. Micro. Sep.* 1999, *11*, 676–681. doi:10.1002/(SICI)1520-667X(199911)11:9<676::AID-MCS5>3.0.CO;2-O

41. Lee, W. J.; Min, B. R.; Moon, M. H. Improvement in Particle Separation by Hollow Fiber Flow Field-Flow Fractionation and the Potential Use in Obtaining Particle Site Distribution. *Anal. Chem.* 1999, *71*, 3446–3452. doi:10.1021/ac981204p

42. Yohannes, G.; Jussila, M.; Hartonen, K.; Riekkola, M. L. Asymmetrical Flow Field-Flow Fractionation Technique for Separation and Characterization of Biopolymers and Bioparticles. *J. Chromatogr. A* 2011, *1218*, 4104–4116. doi:10.1016/j.chroma.2010.12.110

43. Dubascoux, S.; Le Hécho, I.; Hassellöv, M.; Von Der Kammer, F.; Potin Gautier, M.; Lespes, G. Lespes, G. Field-Flow Fractionation and Inductively Coupled Plasma Mass Spectrometer Coupling: History, Development and Applications. *J. Anal. At. Spectrom.* 2010, *25*, 613–623. doi:10.1039/b927500b

44. Marassi, V.; Roda, B.; Zattoni, A.; Tanase, M.; Reschiglian, P. Hollow Fiber Flow Field-Flow Fractionation and Size-Exclusion Chromatography with Multi-Angle Light Scattering

Detection: A Complementary Approach in Biopharmaceutical Industry. *J. Chromatogr. A* 2014, *1372*, 196–203. doi:10.1016/j.chroma.2014.10.072

45. Litzen, A.; Walter, J. K.; Krischollek, H.; Wahlund, K. G. Separation and Quantitation of Monoclonal Antibody Aggregates by Asymmetrical Flow Field-Flow Fractionation and Comparison to Gel-Permeation Chromatography. *Anal. Biochem* 1993, *212*, 469–480. doi: 10.1006/abio.1993.1356

46. Meisterjahn, B.; Wagner, S.; von der Kammer, F.; Hennecke, D.; Hofmann, T. Silver and Gold Nanoparticle Separation Using Asymmetrical Flow-Field Flow Fractionation: Influence of Run Conditions and of Particle and Membrane Charges. *J. Chromatogr. A* 2016, *1440*, 150–159. doi:10.1016/j.chroma.2016.02.059

47. Hagendorfer, H.; Kaegi, R.; Parlinska, M.; Sinnet, B.; Ludwig, C.; Ulrich, A. Characterization of Silver Nanoparticle Products Using Asymmetric Flow Field Flow Fractionation with a Multidetector Approach – A Comparison to Transmission Electron Microscopy and Batch Dynamic Light Scattering. *Anal. Chem.* 2012, *84*, 2678–2685. doi: 10.1021/ac202641d

48. Reschiglian, P.; Melucci, D.; Zattoni, A.; Mallo, L.; Hansen, M.; Kummerow, A.; Miller, M. Working without Accumulation Membrane in Flow Field-Flow Fractionation. *Anal. Chem.* 2000, *72*, 5945–5954. doi:10.1021/ac000608q

49. Bolea, E.; Jimenez-Lamana, J.; Laborda, F.; Castillo, J. R. Size Characterization and Quantification of Silver Nanoparticles by Asymmetric Flow Field-Flow Fractionation Coupled with Inductively Coupled Plasma Mass Spectrometry. *Anal. Bioanal. Chem.* 2011, *401*, 2723–2732. doi:10.1007/s00216-011-5201-2

50. Ramos, K.; Ramos, L.; Cámara, C.; Gómez-Gómez, M. M. Characterization and Quantification of Silver Nanoparticles in Nutraceuticals and Beverages by Asymmetric Flow Field Flow Fractionation Coupled with Inductively Coupled Plasma Mass Spectrometry. *J. Chromatogr. A* 2014, *1371*, 227–236. doi:10.1016/j.chroma.2014.10.060

51. Lee, W.-C.; Lee, B.-T.; Lee, S.; Hwang, Y. S.; Jo, E.; Eom, I.-C.; Lee, S.-W.; Kim, S.-O. Evaluation and Application of Asymmetrical Flow Field-Flow Fractionation with Single Particle Inductively Coupled Plasma Mass Spectrometry (SP-ICP-MS) to Characterise Silver Nanoparticles in Environmental Media. *Microchem. J.* 2016, *129*, 219–230. doi:10.1016/j.microc.2016.06.030

52. Saenmuangchin, R.; Mettakoonpitak, J.; Shiowatana, J.; Siripinyanond, A. Separation of Silver Nanoparticles by Hollow Fiber Flow Field-Flow Fractionation: Addition of Tannic Acid into Carrier Liquid as a Modifier. *J. Chromatogr. A* 2015, *1415*, 115–122. doi:10.1016/j.chroma.2015.08.047

53. Klein, T.; Huerzeler, C. Characterization of Biopolymers, proteins, Particles and Colloids by Means of Field-Flow Fractionation. *GIT Labor. Fachz.* 1999, *11*, 1224–1228.

54. Liu, F. K.; Ko, F. H.; Huang, P. W.; Wu, C. H.; Chu, T. C. Studying the Size/Shape Separation and Optical Properties of Silver Nanoparticles by Capillary Electrophoresis. *J. Chromatogr. A* 2005, *1062*, 139–145. doi:10.1016/j.chroma.2004.11.010

55. Geiss, O.; Cascio, C.; Gilliland, D.; Franchini, F.; Barrero-Moreno, J. Size and Mass Determination of Silver Nanoparticles in an Aqueous Matrix Using Asymmetric Flow Field Flow Fractionation Foupled to Inductively Coupled Plasma Mass Spectrometer and Ultraviolet-Visible Detectors. *J. Chromatogr. A* 2013, *1321*, 100–108. doi:10.1016/j.chroma.2013.10.060

56. Hoque, M. E.; Khosravi, K.; Newman, K.; Metcalfe, C. D. Detection and Characterization of Silver Nanoparticles in Aqueous Matrices Using Asymmetric-Flow Field Flow Fractionation with Inductively Coupled Plasma Mass Spectrometry. *J. Chromatogr. A* 2012, *1233*, 109–115. doi:10.1016/j.chroma.2012.02.011

57. Cho, T. J.; Hackley, V. A. Fractionation and Characterization of Gold Nanoparticles in Aqueous Solution: Asymmetric-Flow Field Flow Fractionation with MALS, DLS, and UV-Vis Detection. *Anal. Bioanal. Chem.* 2010, *398*, 2003–2018. doi:10.1007/s00216-010-4133-6

58. Marassi, V.; Casolari, S.; Roda, B.; Zattoni, A.; Reschiglian, P.; Panzavolta, S.; Tofail, S. A. M.; Ortelli, S.; Delpivo, C.; Blosi, M.; Costa, A. L. Hollow-Fiber Flow Field-Flow

Fractionation and Multi-Angle Light Scattering Investigation of the Size, Shape and Metal-Release of Silver Nanoparticles in Aqueous Medium for Nano-Risk Assessment. *J. Pharm. Biomed. Anal.* 2015, *106*, 92–99. doi:10.1016/j.jpba.2014.11.031

59. Mekprayoon, S.; Siripinyanond, A. Performance Evaluation of Flow Field-Flow Fractionation and Electrothermal Atomic Absorption Spectrometry for Size Characterization of Gold Nanoparticles. *J. Chromatogr. A* 2019, *1604*, 460493. doi:10.1016/j.chroma.2019.460493

60. Hassellov, M.; Lyven, B.; Haraldsson, C.; Sirinawin, W. Determination of Continuous Size and Trace Element Distribution of Colloidal Material in Natural Water by on-Line Coupling of Flow Field-Flow Fractionation with ICPMS. *Anal. Chem.* 1999, *71*, 3497–3502. doi:10.1021/ac981455y

61. Dubascoux, S.; Le Hecho, I.; Gautier, M. P.; Lespes, G. On-Line and off-Line Quantification of Trace Elements Associated to Colloids by as-Fl-FFF and ICP-MS. *Talanta* 2008, *77*, 60–65. doi:10.1016/j.talanta.2008.05.050

62. Loeschner, K.; Navratilova, J.; Legros, S.; Wagner, S.; Grombe, R.; Snell, J.; von der Kammer, F.; Larsen, E. H. Optimization and Evaluation of Asymmetric Flow Field-Flow Fractionation of Silver Nanoparticles. *J. Chromatogr. A* 2013, *1272*, 116–125. doi:10.1016/j.chroma.2012.11.053

63. Meermann, B.; Fabricius, A. L.; Duester, L.; Vanhaecke, F.; Ternes, T. Fraction-Related Quantification of Silver Nanoparticles *via* on-Line Species-Unspecific Post-Channel Isotope Dilution in Combination with Asymmetric Flow-Field-Flow Fractionation (AF4)/ Sector Field ICP-Mass Spectrometry (ICP-SF-MS). *J. Anal. At. Spectrom.* 2014, *29*, 287–296. doi:10.1039/C3JA50179E

64. Sanchez-Cachero, A.; Lopez-Sanz, S.; Farinas, N. R.; Rios, A.; Martin-Doimeadios, R. D. R. A Method Based on Asymmetric Flow Field Flow Fractionation Hyphenated to Inductively Coupled Plasma Mass Spectrometry for the Monitoring of Platinum Nanoparticles in Water Samples. *Talanta* 2021, *222*, 121513.

65. Peng, Z. M.; Yang, H. Designer Platinum Nanoparticles: Control of Shape, Composition in Alloy, Nanostructure and Electrocatalytic Property. *Nano Today* 2009, *4*, 143–164. doi:10.1016/j.nantod.2008.10.010

66. Xu, M.; Soliman, M. G.; Sun, X.; Pelaz, B.; Feliu, N.; Parak, W. J.; Liu, S. J. How Entanglement of Different Physicochemical Properties Complicates the Prediction of *in Vitro* and *in Vivo* Interactions of Gold Nanoparticles. *ACS Nano* 2018, *12*, 10104–10113. doi:10.1021/acsnano.8b04906

67. Dwivedi, A. D.; Dubey, S. P.; Sillanpaa, M.; Kwon, Y. N.; Lee, C.; Varma, R. S. Fate of Engineered Nanoparticles: Implications in the Environment. *Coord. Chem. Rev* 2015, *287*, 64–78. doi:10.1016/j.ccr.2014.12.014

68. Cervantes-Aviles, P.; Huang, Y. X.; Keller, A. A. Incidence and Persistence of Silver Nanoparticles throughout the Wastewater Treatment Process. *Water Res.* 2019, *156*, 188–198. doi:10.1016/j.watres.2019.03.031

69. El Hadri, H.; Louie, S. M.; Hackley, V. A. Assessing the Interactions of Metal Nanoparticles in Soil and Sediment Matrices — A Quantitative Analytical Multi-Technique Approach. *Environ. Sci. Nano* 2018, *5*, 203–214. doi:10.1039/C7EN00868F

70. Liu, H. H.; Bilal, M.; Lazareva, A.; Keller, A.; Cohen, Y. Simulation Tool for Assessing the Release and Environmental Distribution of Nanomaterials. *Beilstein J. Nanotechnol.* 2015, *6*, 938–951. doi:10.3762/bjnano.6.97

71. Koopmans, G. F.; Hiemstra, T.; Regelink, I. C.; Molleman, B.; Comans, R. N. J. Asymmetric Flow Field-Flow Fractionation of Manufactured Silver Nanoparticles Spiked into Soil Solution. *J. Chromatogr. A* 2015, *1392*, 100–109. doi:10.1016/j.chroma.2015.02.073

72. Yi, Z. B.; Loosli, F.; Wang, J. J.; Berti, D.; Baalousha, M. How to Distinguish Natural versus Engineered Nanomaterials: Insights from the Analysis of TiO$_2$ and CeO$_2$ in Soils. *Environ. Chem. Lett.* 2020, *18*, 215–227. doi:10.1007/s10311-019-00926-5

73. Brown, S. D.; Nativo, P.; Smith, J. A.; Stirling, D.; Edwards, P. R.; Venugopal, B.; Flint, D. J.; Plumb, J. A.; Graham, D.; Wheate, N. J. Gold Nanoparticles for the Improved Anticancer Drug Delivery of the Active Component of Oxaliplatin. *J. Am. Chem. Soc.* 2010, *132*, 4678–4684. [Database] doi:10.1021/ja908117a

74. Lapresta-Fernandez, A.; Fernandez, A.; Blasco, J. Nanoecotoxicity Effects of Engineered Silver and Gold Nanoparticles in Aquatic Organisms. *TrAC, Trends Anal. Chem.* 2012, *32*, 40–59. doi:10.1016/j.trac.2011.09.007

75. Judy, J. D.; Unrine, J. M.; Bertsch, P. M. Evidence for Biomagnification of Gold Nanoparticles within a Terrestrial Food Chain. *Environ. Sci. Technol.* 2011, *45*, 776–781. doi:10.1021/es103031a

76. Krystek, P.; Brandsma, S.; Leonards, P.; de Boer, J. Exploring Methods for Compositional and Particle Size Analysis of Noble Metal Nanoparticles in *Daphnia Magna*. *Talanta* 2016, *147*, 289–295. doi:10.1016/j.talanta.2015.09.063

77. Krystek, P.; Kettler, K.; van der Wagt, B.; de Jong, W. H. Exploring Influences on the Cellular Uptake of Medium-Sized Silver Nanoparticles into THP-1 Cells. *Microchem. J.* 2015, *120*, 45–50. doi:10.1016/j.microc.2015.01.005

78. Cedervall, T.; Lynch, I.; Lindman, S.; Berggard, T.; Thulin, E.; Nilsson, H.; Dawson, K. A.; Linse, S. Understanding the Nanoparticle-Protein Corona Using Methods to Quantify Exchange Rates and Affinities of Proteins for Nanoparticles. *Proc. Natl. Acad. Sci. USA* 2007, *104*, 2050–2055. doi:10.1073/pnas.0608582104

79. Walkey, C. D.; Olsen, J. B.; Song, F. Y.; Liu, R.; Guo, H. B.; Olsen, D. W. H.; Cohen, Y.; Emili, A.; Chan, W. C. W. Protein Corona Fingerprinting Predicts the Cellular Interaction of Gold and Silver Nanoparticles. *ACS Nano* 2014, *8*, 2439–2455. doi:10.1021/nn406018q

80. Xu, L. N.; Xu, M.; Wang, R. X.; Yin, Y. G.; Lynch, I.; Liu, S. J. The Crucial Role of Environmental Coronas in Determining the Biological Effects of Engineered Nanomaterials. *Small* 2020, *16*, 2003691. doi:10.1002/smll.202003691

81. Wimuktiwan, P.; Shiowatana, J.; Siripinyanond, A. Investigation of Silver Nanoparticles and Plasma Protein Association Using Flow Field-Flow Fractionation Coupled with Inductively Coupled Plasma Mass Spectrometry (FlFFF-ICP-MS.).*J. Anal. At. Spectrom.* 2015, *30*, 245–253. doi:10.1039/C4JA00225C

82. Lopez-Sanz, S.; Rodriguez Farinas, N.; Martin-Doimeadios, R. D. R.; Rios, A. Analytical Strategy Based on Asymmetric Flow Field Flow Fractionation Hyphenated to ICP-MS and Complementary Techniques to Study Gold Nanoparticles Transformations in Cell Culture Medium. *Anal. Chim. Acta* 2019, *1053*, 178–185.

83. Liu, W.; Worms, I. A. M.; Herlin-Boime, N.; Truffier-Boutry, D.; Michaud-Soret, I.; Mintz, E.; Vidaud, C.; Rollin-Genetet, F. Interaction of Silver Nanoparticles with Netallothionein and Ceruloplasmin: Impact on Metal Substitution by Ag(I), Corona Formation and Enzymatic Activity. *Nanoscale* 2017, *9*, 6581–6594. doi:10.1039/C7NR01075C

84. Delay, M.; Dolt, T.; Woellhaf, A.; Sembritzki, R.; Frimmel, F. H. Interactions and Stability of Silver Nanoparticles in the Aqueous Phase: Influence of Natural Organic Matter (NOM) and Ionic Strength. *J. Chromatogr. A* 2011, *1218*, 4206–4212. doi:10.1016/j.chroma.2011.02.074

85. Tan, Z. Q.; Yin, Y. G.; Guo, X. R.; Amde, M.; Moon, M. H.; Liu, J. F.; Jiang, G. B. Tracking the Transformation of Nanoparticulate and Ionic Silver at Environmentally Relevant Concentration Levels by Hollow Fiber Flow Field-Flow Fractionation Coupled to ICPMS. *Environ. Sci. Technol.* 2017, *51*, 12369–12376. doi:10.1021/acs.est.7b03439

86. Liu, X. S.; Chen, Y. J.; Li, H.; Huang, N.; Jin, Q.; Ren, K. F.; Ji, J. Enhanced Retention and Cellular Uptake of Nanoparticles in Tumors by Controlling Their Aggregation Behavior. *ACS Nano* 2013, *7*, 6244–6257. doi:10.1021/nn402201w

87. Guo, H. Y.; Xing, B. S.; He, L. L. Development of a Filter-Based Method for Detecting Silver Nanoparticles and Their Heteroaggregation in Aqueous Environments by Surface-Enhanced Raman Spectroscopy. *Environ. Pollut.* 2016, *211*, 198–205. doi:10.1016/j.envpol.2015.12.049

88. Wang, C.; Lv, B. W.; Hou, J.; Wang, P. F.; Miao, L. Z.; Ci, H. L. Quantitative Measurement of Aggregation Kinetics Process of Nanoparticles Using Nanoparticle Tracking Analysis and Dynamic Light Scattering. *J. Nanopart. Res.* 2019, *21*, 87.

89. Kim, S. T.; Lee, Y. J.; Hwang, Y. S.; Lee, S. Study on Aggregation Behavior of Cytochrome C-Conjugated Silver Nanoparticles Using Asymmetrical Flow Field-Flow Fractionation. *Talanta* 2015, *132*, 939–944. doi:10.1016/j.talanta.2014.05.060

90. Pamies, R.; Cifre, J. G. H.; Espin, V. F.; Collado-Gonzalez, M.; Banos, F. G. D.; de la Torre, J. G. Aggregation Behaviour of Gold Nanoparticles in Saline Aqueous Media. *J. Nanopart. Res.* 2014, *16*, 2376.

91. Yin, Y. G.; Yang, X. Y.; Zhou, X. X.; Wang, W. D.; Yu, S. J.; Liu, J. F.; Jiang, G. B. Water Chemistry Controlled Aggregation and Photo-Transformation of Silver Nanoparticles in Environmental Waters. *J. Environ. Sci.* 2015, *34*, 116–125. doi:10.1016/j.jes.2015.04.005

92. Antonio, D. C.; Cascio, C.; Jaksic, Z.; Jurasin, D.; Lyons, D. M.; Nogueira, A. J. A.; Rossi, F.; Calzolai, L. Assessing Silver Nanoparticles Behaviour in Artificial Seawater by Mean of AF4 and spICP-MS. *Mar. Environ. Res.* 2015, *111*, 162–169. doi:10.1016/j.marenvres.2015.05.006

93. Stankus, D. P.; Lohse, S. E.; Hutchison, J. E.; Nason, J. A. Interactions between Natural Organic Matter and Gold Nanoparticles Stabilized with Different Organic Capping Agents. *Environ. Sci. Technol.* 2011, *45*, 3238–3244. doi:10.1021/es102603p

94. Sikder, M.; Wang, J. J.; Poulin, B. A.; Tfaily, M. M.; Baalousha, M. Nanoparticle Size and Natural Organic Matter Composition Determine Aggregation Behavior of Polyvinylpyrrolidone Coated Platinum Nanoparticles. *Environ. Sci: Nano* 2020, *7*, 3318–3332. doi:10.1039/D0EN00659A

95. Yin, Y. G.; Shen, M. H.; Tan, Z. Q.; Yu, S. J.; Liu, J. F.; Jiang, G. B. Particle Coating-Dependent Interaction of Molecular Weight Fractionated Natural Organic Matter: Impacts on the Aggregation of Silver Nanoparticles. *Environ. Sci. Technol.* 2015, *49*, 6581–6589. doi:10.1021/es5061287

96. Motellier, S.; Pelissier, N.; Mattei, J. G. Aging of Silver Nanocolloids in Sunlight: Particle Size Has a Major Influence. *Environ. Chem.* 2018, *15*, 450–462. doi:10.1071/EN18056

97. Klitzke, S.; Metreveli, G.; Peters, A.; Schaumann, G. E.; Lang, F. The Fate of Silver Nanoparticles in Soil Solution — Sorption of Solutes and Aggregation. *Sci. Total Environ.* 2015, *535*, 54–60. doi:10.1016/j.scitotenv.2014.10.108

98. Zhang, W. C.; Xiao, B. D.; Fang, T. Chemical Transformation of Silver Nanoparticles in Aquatic Environments: Mechanism, Morphology and Toxicity. *Chemosphere* 2018, *191*, 324–334. doi:10.1016/j.chemosphere.2017.10.016

99. Furtado, L. M.; Hoque, M. E.; Mitrano, D. F.; Ranville, J. F.; Cheever, B.; Frost, P. C.; Xenopoulos, M. A.; Hintelmann, H.; Metcalfe, C. D. The Persistence and Transformation of Silver Nanoparticles in Littoral Lake Mesocosms Monitored Using Various Analytical Techniques. *Environ. Chem.* 2014, *11*, 419–430. doi:10.1071/EN14064

100. Yin, Y. G.; Liu, J. F.; Jiang, G. B. Sunlight-Induced Reduction of Ionic Ag and Au to Metallic Nanoparticles by Dissolved Organic Matter. *ACS Nano* 2012, *6*, 7910–7919. doi:10.1021/nn302293r

101. Levard, C.; Reinsch, B. C.; Michel, F. M.; Oumahi, C.; Lowry, G. V.; Brown, G. E. Sulfidation Processes of PVP-Coated Silver Nanoparticles in Aqueous Solution: Impact on Dissolution Rate. *Environ. Sci. Technol.* 2011, *45*, 5260–5266. doi:10.1021/es2007758

102. Pettibone, J. M.; Gigault, J.; Hackley, V. A. Discriminating the Sates of Matter in Metallic Nanoparticle Transformations: What Are We Missing? *ACS Nano* 2013, *7*, 2491–2499. doi:10.1021/nn3058517

103. Pettibone, J. M.; Liu, J. Y. Sin Situ Methods for Monitoring Silver Nanoparticle Sulfidation in Simulated Waters. *Environ. Sci. Technol.* 2016, *50*, 11145–11153. doi:10.1021/acs.est.6b03023